Metallurgical technologies / Металлургические технологии

UDC 669.162
DOI 10.17073/0368-0797-2024-1-19-26

Original article
Оригинальная статья

Possibilities of heat-power spraying of wet charge during formation of structural properties of agglomerated iron ore materials

V. M. Pavlovets

Siberian State Industrial University (42 Kirova Str., Novokuznetsk, Kemerovo Region – Kuzbass 654007, Russian Federation)

pawlowets.victor@yandex.ru

Abstract. The substantiated problem of improving the structural properties of agglomerated metallurgical raw materials is associated with the formation of a favorable pore structure in iron ore pellets. The author analyzed various methods for the formation of structural properties of molded dispersed materials in various industries. The paper presents the technological capabilities of promising technologies for production of iron ore pellets based on the heat-power spraying of wet charge on pelletizer's charge skull and pelletized materials. The physical possibilities of heat-power spraying of wet charge in the forced nucleation and in the process of forming the iron ore pellets' structural properties are disclosed at the stage of pelletizing. The technical features and production operations of the main technologies for wet charge spraying and the design features of devices for obtaining pellets are shown. The paper describes the experimental unit and technology for the forced nucleation. The macro- and microstructure of the germ mass at forced nucleation were studied. Principles of the formation of regulated structure and improved metallurgical properties in iron ore pellets were substantiated. The article presents the description and characteristics of structural changes on the surface of the sprayed charge layer. A hypothesis was put forward about the structural correspondence of geometric dimensions and relief of charge lappings and cavities in the sprayed layer with the nature of porosity and germ structure. The germ mass affects the pellets' structural properties. The author obtained the dependences of structural changes' relative values on the sprayed layer surface on pressure of air-charge jet and particle size of the sprayed charge. There is relationship between geometric dimensions of the sprayed charge layer and the structural changes' size. A probable mechanism of porosity formation in the germ mass during heat-power spraying of a wet charge onto the pelletizer skull was formulated. The aerodynamic characteristics of air-charge jet influence the formation of porosity. New possibilities of heat-power spraying of wet charge can intensify pellets production and improve their quality.

Keywords: structural properties, agglomerated metallurgical raw materials, iron ore pellets, thermal-power heat-power spraying of wet charge, germ mass, forced nucleation

For citation: Pavlovets V.M. Possibilities of heat-power spraying of wet charge during formation of structural properties of agglomerated iron ore materials. *Izvestiya. Ferrous Metallurgy*. 2024;67(1):19–26. https://doi.org/10.17073/0368-0797-2024-1-19-26

Возможности теплосилового напыления влажной шихты в процессе формирования структурных свойств окускованных железорудных материалов

В. М. Павловец

Сибирский государственный индустриальный университет (Россия, 654007, Кемеровская обл. – Кузбасс, Новокузнецк, ул. Кирова, 42)

pawlowets.victor@yandex.ru

Аннотация. Повышение структурных свойств окускованного металлургического сырья за счет формирования благоприятной поровой структуры у железорудных окатышей является актуальной задачей. Методы формирования структурных свойств у сформованных дисперсных материалов проанализированы применительно к различным отраслям промышленности. В работе представлены технологические возможности перспективных технологий производства железорудных окатышей на основе теплосилового напыления влажной шихты на шихтовый гарнисаж окомкователя и комкуемые материалы. Теплосиловое напыление влажной шихты в технике принудительного зародышеобразования позволяет формировать структурные свойства железорудных окатышей на стадии окомкования. Конструктивные особенности устройств для получения окатышей зависят от применяемых производственных технологий напыления влажной шихты на ограждения окомкователя. Методики экспериментов зависят от техники принудительного зародышеобразования. Технологии принудительного зародышеобразования влияют на макро- и микроструктуры зародышевой массы. Принципы регламентированного структурообразования позволяют формировать улучшенные металлургические свойства окатышей. На поверхности напыленного слоя шихты образуются структурные изменения в форме углублений и шихтовых наплывов. Высказана гипотеза о структурном соответствии геометрических размеров, рельефа шихтовых наплывов и углублений у напыленного слоя с характером пористости и структуры зародышей. Количество зародышевой массы внутри окатышей влияет на их структурные свойства. Относительная величина структурных изменений на поверхности напыленного слоя шихты и их количество определяются давлением воздушношихтовой струи и размером напыляемых частиц. Вероятный механизм формирования пористости зародышевой массы в процессе теплосилового напыления влажной шихты на гарнисаж окомкователя зависит от параметров технологии. Обоснован сдвиговый механизм образования открытой пористости в структуре зародышевой массы. Аэродинамические характеристики воздушношихтовой струи влияют на формирование пористости. Новые технологии теплосилового напыления влажной шихты позволяют интенсифицировать производство и улучшать качество окатышей.

Ключевые слова: структурные свойства, окускованное металлургическое сырье, железорудные окатыши, теплосиловое напыление влажной шихты, зародышевая масса, технология принудительного зародышеобразования

Для цитирования: Павловец В.М. Возможности теплосилового напыления влажной шихты в процессе формирования структурных свойств окускованных железорудных материалов. *Известия вузов. Черная металлургия*. 2024;67(1):19–26.
https://doi.org/10.17073/0368-0797-2024-1-19-26

Introduction

Various techniques, including intensive modes of heat treatment, foaming, combustible additives, special pore-forming and ore-forming compositions, and other materials, are used to determine special structural properties of the majority of molded porous products across various branches of engineering, such as metallurgy, the manufacture of refractory products, construction operations, etc. [1 – 3]. The increased requirements to pelletized metallurgical raw materials in terms of iron content considerably limit the application of pore-forming additives and expand the use of methods for forming pores in the structure of iron ore pellets [4 – 7]. One way to improve the structural properties of pellets without using pore-forming additives is to apply a two-step technology. One of its steps enables the formation of most of the pellet mass by heat-power spraying of wet charge at the pelletizing stage [8; 9]. As a structure- and form-forming energy carrier, this technology uses an air charge jet (ACJ) based on cold or heated up to 100 – 150 °C compressed air, which enables the formation of a wet charge sprayed layer (SL) on almost any technological surface [8; 9]. The raw pellets production based on the spraying technique also includes the operations of charge pelletizing and after-pelletizing of germs. Numerous experimentally proven combined technologies have been successfully explored in laboratories and have shown high practical efficiency [8; 9]. Some technical indicators of the mentioned technologies, in comparison with the traditional method, are given in the Table below [8 – 10].

Flow schemes for pellets production based on heat-power spraying of wet charge onto the charge skull of the plate pelletizer are illustrated in Fig. 1, *a*. The spraying schemes for pelletized materials are depicted in Fig. 1, *b*, *c*. The process of pellet production employing the forced nucleation technology (NSA) has been most thoroughly investigated under laboratory conditions. This technique involves forming the germinal

Technical indicators of pelletizing technologies

Технические показатели технологий получения окатышей

Technical indicators	Pelletizing technologies			
	NP	NSA	NPSA	NPS
Spraying area, % of the plate area	–	30 – 40	20 – 30	15 – 25
Area occupied by pelletized materials, %	40 – 50	70 – 90	50 – 55	40 – 50
Relative productivity, %	100	115 – 130	105 – 115	110 – 120
Weight percentage of sprayed material in the pellet structure, %	–	up to 70	up to 40	up to 50
Spraying efficiency, %	–	up to 90	up to 70	up to 60
Pellet weight growth rate, g/s	0.01 – 0.03	0.08 – 0.24	0.05 – 0.14	0.08 – 0.31
Dehumidification of pellets after pelletizing, %	–	0.4 – 1.2	0.4 – 1.0	0.5 – 0.9
Moisture removal intensity in the process of nucleation, kg/(m^2·s)	–	$(4 – 8)\cdot 10^{-3}$	$(5 – 10)\cdot 10^{-3}$	$(5 – 10)\cdot 10^{-3}$
Crack formation temperature, °C	550 – 580	600 – 740	580 – 650	580 – 620
Total porosity of pellets, %	23 – 28	28 – 35	26 – 32	28 – 34
Number of open pores, %	20 – 25	25 – 30	22 – 26	24 – 28
Relative strength of pellets, %	100	90 – 110	90 – 100	85 – 95

part of pellets and their pore structure through heat-power spraying of wet charge onto the bottom charge skull in the idle zone of the pelletizer (Fig. 1, *a*) [8; 9]. Using this technique, the SL and germs exhibit reduced moisture content and a favorable pore structure, characterized by an increased number (up to 40 %) of open pores with low tortuosity [9]. The operations to produce suitable pellets include the mechanical division of SL into germs, spheroidization of germs, and their after-pelletizing in the rerolling mode. The NSA technology enables the achievement of superior performance characteristics and pellet properties (refer to the table). In the NPS and NPSF technologies, the germs are small pellets ranging in size from 4 to 12 mm. According to the NPSF technology, as the pellet mass forms, an internal charge sprayed layer is created on the surfaces of 4 – 7 mm germs, positioned between the germ and the shell. The mass of the sprayed layer can account for up to 40 % of the total (Fig. 1, *b*). During the NPS process, the pellet shell forms on the surfaces of larger pellets, 8 – 12 mm in size, that are grouped in the circulation zone of the pelletizer by spraying wet material onto the pelletized materials. Here, spraying serves as a finishing technique, after which the pellets achieve their standard size (14 – 16 mm) (Fig. 1, *c*). The strength of the surface shell can be increased by 5 – 15 % compared to the traditional industrial NP technology, albeit at the expense of some structural characteristics of the pellets. When employing these technologies, the germ mass is formed by pelletizing the wet charge in the rerolling mode, eliminating the need for mechanical follow-up elements. However, the efficiency of spraying, the weight percentage of the sprayed layer in the pellets, and some process specifications slightly lag behind the NSA technique. The processes developed can be easily integrated into existing facilities with minimal adjustments. Additionally, if needed, reverting to the conventional technology (NP), which relies on wet charge drip nucleation followed by after-pelletizing in the rerolling mode, is straightforward.

The spraying technique is extensively utilized across various manufacturing processes [11; 12], enabling the formation of structural properties in a broad array of sprayed materials [13 – 15]. Technologies based on spraying offer several technical benefits and are distinguished by numerous control actions, both in the manufacturing process itself and in terms of enhancing and broadening the consumer properties of the processed products. This is especially relevant to pellet production, where the technique of wet charge spraying using an air charge jet (ACJ) opens significant potential for influencing the structure of germs and pellets [8 – 10].

The aim of this paper is to explore the mechanism of structure formation in the germinal centers of pellets produced through the technology of heat-power spraying of wet charge onto the pelletizer's bottom skull.

Materials and methods

The experiments were conducted on a laboratory semi-industrial pelletizer with a diameter of 0.62 m, inclined at a 45° angle to the horizon, and rotating at a speed of 12 rpm. The sprayed charge, with a moisture content of 5.0; 7,5; 10.0 %, consisted of iron ore concentrate from the Teysk deposit and 1 % of bentonite as a binder. The wet charge was sprayed onto the charge skull using compressed air at a pressure of 0.2 MPa and a flow rate of 0.6 m^3/min. After spraying, the geometric dimensions of the SL were measured. Samples taken from the SL using the cutting ring method (GOST 5180 – 84) were utilized to evaluate compressive strength (GOST 17245 – 79

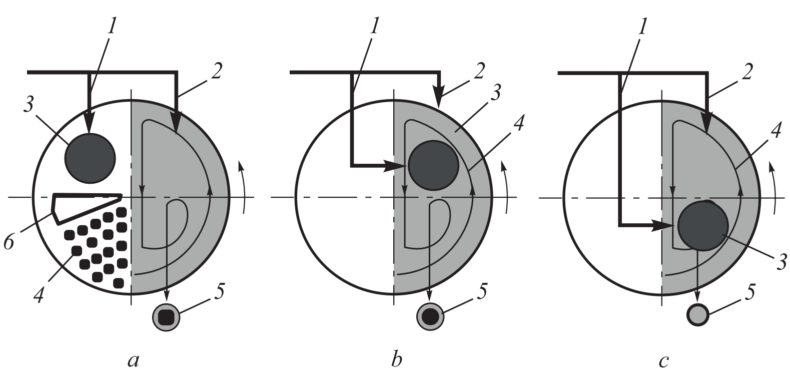

Fig. 1. Schemes for obtaining pellets based on heat-power spraying of wet charge on the charge scull of a plate pelletizer (*a*) and pelletized materials (*b*, *c*):
1, *2* – independent flows of the loaded charge; *3* – sprayed layer (*a*), spraying area (*b*, *c*) in the layer of pelletized materials; *4* – germs; *5* – suitable pellets; *6* – divider of sprayed layer (SL)

Рис. 1. Схемы получения окатышей на основе теплосилового напыления влажной шихты на шихтовый гарнисаж тарельчатого окомкователя (*a*) и комкуемые материалы (*b*, *c*):
1, *2* – самостоятельные потоки загружаемой шихты; *3* – напыленный слой (*a*) и область напыления (*b*, *c*) в слое комкуемых материалов; *4* – зародыши; *5* – годные окатыши; *6* – делитель НС

and 26447 – 85) and density. In each SL zone, defined by a relative diameter δ equal to 0 ± 0.2, samples were collected with samplers (cutting ring) 10 mm in diameter, amounting to 10 – 15 samples per zone. The procedure is elaborated upon in references [8; 9]. The analysis of the germ structure formation mechanism during heat-power spraying of charge focused on:

– the macrostructure of the SL surface formed after spraying;

– the surface microstructure of the SL samples on their horizontal plane parallel to the sprayed base and on their vertical plane perpendicular to the sprayed base (Fig. 2).

Samples for microstructure analysis were fired in an electric furnace at 800 °C.

Structural alterations on the surface of the sprayed charge layer included cavities and charge lappings, arising from the dynamic impact of the ACJ on the SL surface. This interaction results in the formation of a wave-like relief on the surface, characterized by alternating cavities and lappings (Fig. 2, *a*, *b*, *c*). These structural changes, with varying geometric dimensions, shapes, locations, and tortuosities, serve as external indicators of the process, facilitating the analysis of pore formation within the germ [8]. Structural cavities in the SL are concentric channels with low tortuosity, arranged along a circular path between charge lappings around the axis of the circular SL, with the jet angle of attack (β) set to 90°. These channels often form a loop, with some being intermittent. In macrostructure photographs, they appear as dark

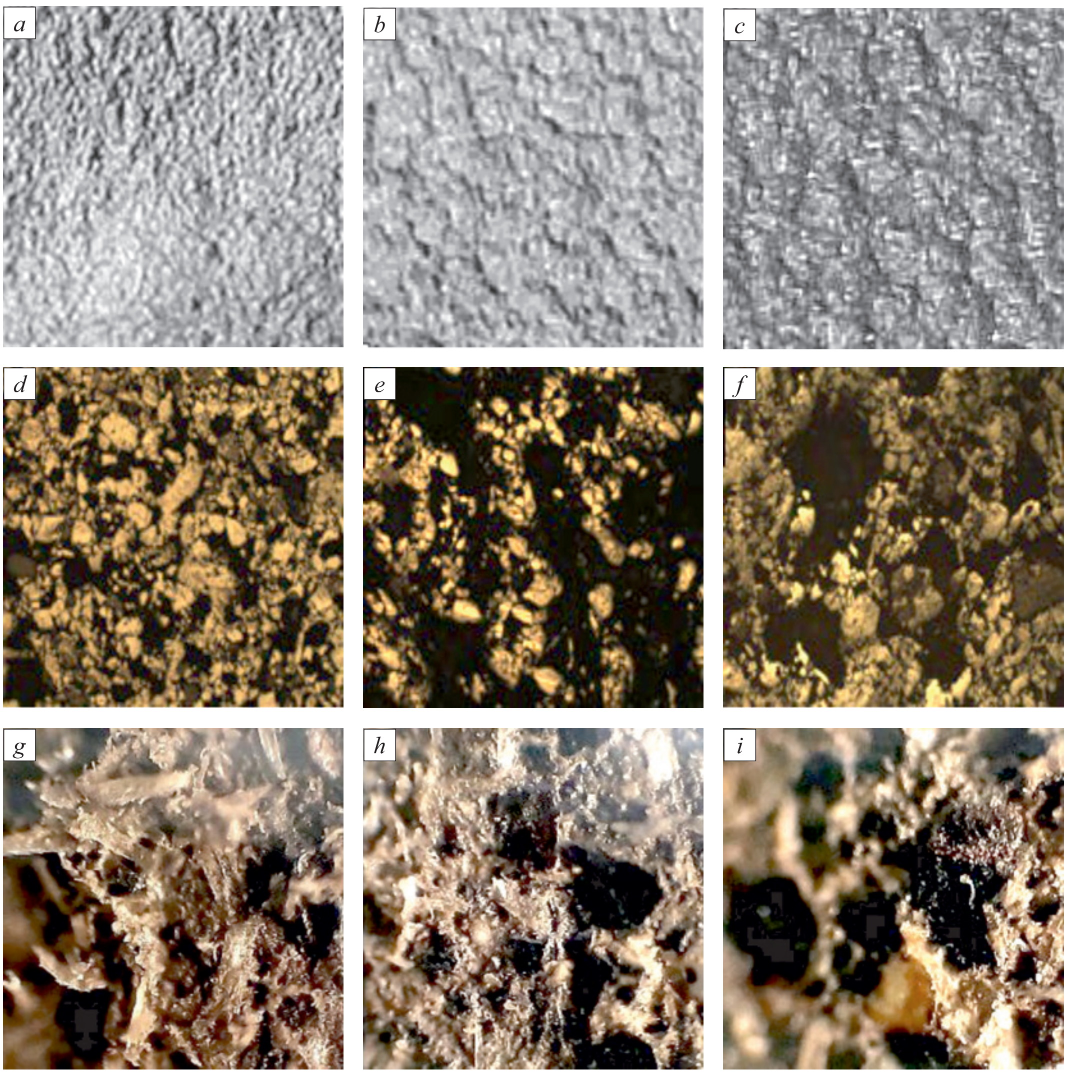

Fig. 2. Macrostructure and microstructure of SL surface after spraying on horizontal and vertical planes of the samples:
a, *b*, *c* – SL surface, ×10; *d*, *e*, *f* – thin section in the horizontal plane, ×100; *g*, *h*, *i* – thin section in the vertical plane, ×100;
a, *d*, *g* – SL central zone δ = 0; β = 90°; *b*, *e*, *h* – intermediate zone δ = 0.5; β = 90°; *c*, *f*, *i* – peripheral zone δ = 0.7; β = 90°

Рис. 2. Макроструктура поверхности НС после напыления и микроструктуры поверхности образцов НС на горизонтальной и вертикальной плоскостях образцов:
a, *b*, *c* – поверхность НС, ×10; *d*, *e*, *f* – поверхность шлифа в горизонтальной плоскости, ×100;
g, *h*, *i* – поверхность шлифа в вертикальной плоскости, ×100; *a*, *d*, *g* – центральная зона НС, δ = 0, β = 90°;
b, *e*, *h* – промежуточная зона, δ = 0,5, β = 90°; *c*, *f*, *i* – периферийная зона, δ = 0,7, β = 90°

lines ranging from 0.1 to 2.5 mm in width. The charge lappings, in contrast, are wider, measuring 1 to 5 mm across. They feature a sloping surface on the side facing the ACJ attack and a steep slope on the opposite (shadow) side. These structural changes make it possible to establish a structural congruence between the SL surface relief and the pore structure of the germ mass [8]. Such surface formations of sprayed coatings have attracted the attention of both domestic [16; 17] and international researchers [18 – 21].

For analyzing the SL macrostructure, two parameters were employed: the relative value of the structural cavities of the SL θ_{ho} and the relative number of structural cavities θ_N, amount/m² (1/m²), on its surface. The relative width of the structural cavities can be determined using the expression

$$\theta_{ho} = \frac{h_o}{h},$$

where h_o is the average width of structural cavities, mm; h is the average height of the sprayed layer on its axis, mm.

The relative number of structural cavities is calculated using the expression

$$\theta_N = \frac{N}{f_{SL}},$$

where N is the average number of structural cavities, determined by the number of concentric shadow channels in the SL; f_{SL} is the area of the SL with a diameter of d, m².

The technique of measuring structural changes is detailed in [9]. These parameters, θ_{ho} and θ_N, are evaluated in relation to variables such as the ACJ pressure P_{ACJ}, moisture content W_c and the average particle size d_p of the sprayed charge. The ACJ pressure is determined based on a nomographic chart that considers both the charge parameters and the characteristics of the jet device [8].

Results and discussion

The experimental findings are depicted in Figs. 3 and 4. Specifically, the parameter θ_{ho} shows a marked decrease as the ACJ pressure increases to 800 Pa, beyond which it declines more gradually (Fig. 4, *a*). with increasing ACJ pressure, the dimensions of structural cavities diminish, while concurrently, the average height of the sprayed layer on its axis expands (Fig. 3). A similar impact is observed with the reduction in particle size of the sprayed charge on the SL's structural parameters (Fig. 4, *b*), where the rate of decrease in h_o outpaces the growth in the sprayed layer's height h. This implies a significant influence of both the moisture content of the sprayed charge and the presence of mobile charge pulp (hydromix) on the surface of the SL, which is generated when the charge mixes with water expelled from the depth to the surface of the SL by the ACJ pressure [8]. At a low moisture content W_c = 5.0 % and an ACJ pressure of 200 Pa and higher, it is postulated that charge pulp is not formed in this mode of spraying, thereby not affecting the structure formation of the SL. In such conditions, the surface of the SL predominantly features low lappings and small structural cavities (h_o < 0.1 – 0.2 mm), whose dimensions can be measured and analyzed under sufficient magnification. Conversely, at a moisture content of W_c = 7.5 %, the quantity of mobile charge pulp increases during spraying, leading to a decrease in the viscosity of the charge on the surface. This condition facilitates the creation of larger charge lappings and structural cavities, which become visually observable. As the ACJ pressure exceeds 800 – 1000 Pa and the charge moisture content reaches W_c = 10.0 %, there is a significant increase in the amount of mobile charge pulp of lower viscosity. This pulp readily fills the cavities, leading to the formation of a relatively uniform structural relief on the surface of the SL with a plethora of small pore channels. The appearance of charge pulp on the surface during the pellet production process serves as an indicator of impact pelletization, a phenomenon where the physical impact of spraying influences the formation and characteristics of pellets [1; 4]. Interestingly, the pattern of these findings bears resemblance to those observed in the plasma spraying of metal powders [16; 17].

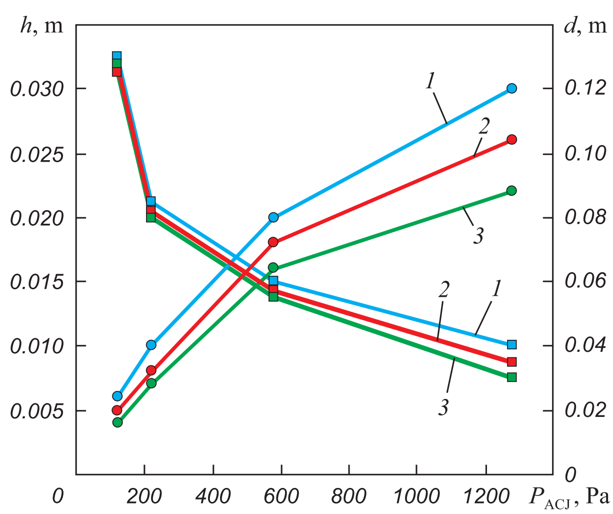

Fig. 3. Dependence of the average height (●, ●, ●) and diameter of the sprayed layer of charge (■, ■, ■) on pressure of air-charge jet (ACJ), moisture content of the charge: *1* – 10.0 %; *2* – 7.5 %; *3* – 5.0 % at the average charge particle size of 0.068 mm

Рис. 3. Зависимость средней высоты (●, ●, ●) и диаметра напыленного слоя шихты (■, ■, ■) от давления ВШС при влажности шихты: *1* – 10,0 %; *2* – 7,5 %; *3* – 5,0 %, средний размер частиц шихты 0,068 мм

The parameter θ_N, which represents the relative number of concentric structural cavities on the surface of the SL, varies with P_{ACJ} pressure (Fig. 4). A notable increase in θ_N nearly fourfold, is observed as the charge moisture content rises from 5.0 to 10.0 % at a P_{ACJ} = 1280 Pa. This phenomenon is attributed to the increased ACJ pressure, which not only escalates the number of structural cavities but does so at a rate much faster than the growth in the diameter d of the SL and its area f_{SL} (Fig. 3). Under these conditions, the mobile charge pulp is capable of flowing into adjacent zones of the SL in the direction of the air movement, consequently altering the size of cavities on the SL surface.

Analyzing the parameter θ_F, which is defined as the ratio of the sizes of structural cavities to the surface area of the sprayed layer ($\theta_F = h_o/F$, m^{-1}), reveals that at a moisture content of 10.0 % θ_F remains constant across a wide range of ACJ pressures, maintaining a value of 0.1. This consistency in θ_F suggests that the ACJ pressure proportionally affects both the sizes of structural cavities and the dimensions of the sprayed layer (SL) itself. In contrast, for sprayed charges with moisture contents of 7.5 and 5.0 %, θ_F decreases to 0.07 and 0.05, respectively, within the same ACJ pressure range. This indicates that the formation of the SL's shape and structure from charges with lower moisture content is significantly less favorable compared to those with higher moisture content due to the smaller sizes of cavities and lappings. As the moisture content of the charge increases, so do the mass and dimensions of the SL, leading to its expansion over a larger area and the enlargement of lappings and cavities. Conversely, with decreasing charge moisture, the mass, diameter, and height of the SL grow at a slower pace, resulting in smaller lappings and cavities. However, the number and concentration of these features within the area F increase, as structural cavities become more densely packed. It is noted that starting from ACJ pressures of 800 – 1000 Pa, the geometric dimensions of lappings and cavities decrease regardless of the moisture content.

The formation of air cavities (pores) on the surface of the SL is most likely to occur at the base of the structural cavities, where the adhesion of the charge lapping to the sprayed base is at its strongest. Under the influence of ACJ pressure, the crest of the lapping, being more mobile due to its specific geometric shape, is subjected to greater deformation. This mobility and deformability allow the lapping crest to potentially block voids in areas that are inaccessible to ACJ pressure. If the charge lappings lack sufficient mobility for this first mechanism of pore formation to take place, an alternative mechanism can occur, whereby voids are formed through the mechanical overlapping of structural cavities by the sprayed charge. The feasibility of this mechanism of structure formation has been supported by research findings pre-

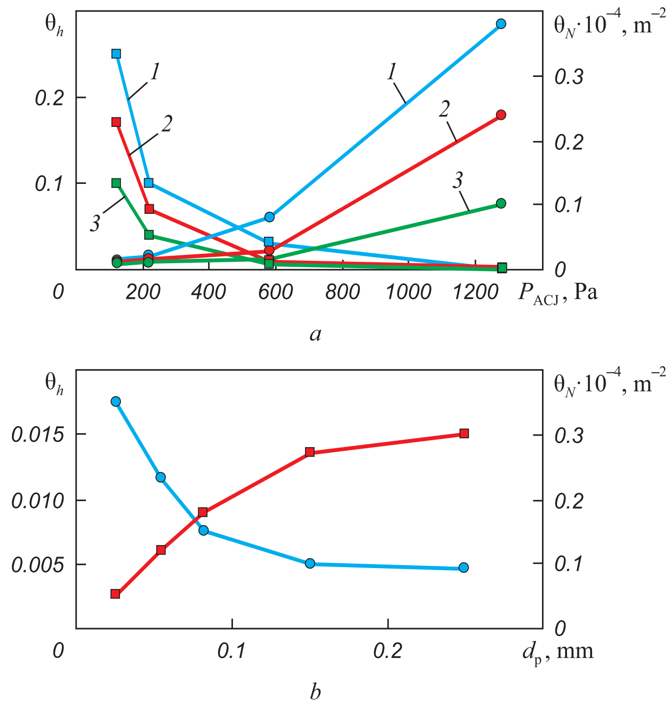

Fig. 4. Dependence of the relative size (●, ●, ●) and relative number of structural cavities of the sprayed charge layer (■, ■, ■) on pressure of ACJ at moisture content of the charge: *1* – 10.0 %; *2* – 7.5 %; *3* – 5.0 % (*a*) and average particle size at P_{ACJ} = 580 Pa, W_c = 10.0 % (*b*), the average charge particle size of 0.068 mm

Рис. 4. Зависимость относительной величины структурных углублений (●, ●, ●) и относительного количества структурных углублений напыленного слоя шихты (■, ■, ■) от давления ВШС при влажности шихты: *1* – 10,0 %; *2* – 7,5 %; *3* – 5,0 % (*a*) и среднего размера частиц при P_{ACJ} = 580 Па, W_c = 10,0 % (*b*), средний размер частиц шихты 0,068 мм

sented in publications [8; 9]. These studies have demonstrated that defects in pellets and irregularities in the SL can be mitigated through the application of a hardening charge coating created by gas spraying. During the spraying process, the ACJ not only applies to the surface but also exerts dynamic shear forces on the deeper layers of the SL, extending from its axis to its periphery. It is this action that is believed to lead to the emergence of elongated pore channels (Fig. 2, *g*, *h*, *i*) which contributes to the formation of open pores within the germ structure. Interestingly, these pores are oriented with a slight inclination in the direction opposite to the ACJ's point of impact.

In the central zone of the SL, channels are densely packed and exhibit minimal sizes, a characteristic attributed to the high-velocity force pressure of the ACJ moving across the SL surface and the increased fluidity of the mobile charge pulp extruded from the SL's depth to its surface. This same mechanism is implicated in the formation of porosity within the depth of the SL. The aggregation of the SL undergoes shear power loads due to the dynamic pressure of the ACJ, which is directed from the SL axis towards the periphery, leading to a characteristic inclination of the pores in the direction opposite to the jet's attack. In the intermediate zone of the SL, where the ACJ dynamic pressure reaches its maximum, cavities become larger but much shorter, and their tortuosity and density increase. This zone also features a mix of open pores and a smaller number of irregularly shaped, closed-type pores. Towards the peripheral zone of the SL, total porosity significantly rises, with the number of channel-type pores sharply decreasing and only forming at the beginning of the zone. The pores at the end of this zone are predominantly of the closed type, larger, and their longitudinal and transverse dimensions vary substantially. To enhance the structural uniformity of germs in the SL peripheral zone and reduce the sizes of structural cavities and overall porosity of the sprayed mass, certain techniques have been suggested. These include increasing the charge moisture content, employing multi-jet spraying, and introducing stabilizing additives into the ACJ [8; 9]. The continued influence of the ACJ on the SL suggests that structure formation within its depth, regarding changes in pore sizes, their configuration, and spheroidization, can persist. The elongated shape of pores in the SL's horizontal cross-section (Fig. 2, *d*, *e*, *f*), which closely mirrors the projection of structural cavities on the SL surface (Fig. 2, *a*, *b*, *c*) indirectly supports this mechanism of structure formation. However, the complexity of these processes, occurring dynamically within a closed system and potentially influenced by the force effect of production unit enclosures and other related phenomena [22; 23]. As these processes occurring in the dynamic state in the closed system are complex and multifaceted, all the described mechanisms of structure formation are probabilistic in nature.

Conclusions

The paper effectively elucidates the impact of heat-power spraying of wet charge on the intensification of production processes and the formation of structural properties of iron ore pellets. By presenting detailed investigations into the macro- and microstructures of germs, the study highlights the application of forced nucleation technology as a method to regulate structure formation and improve the metallurgical properties of iron ore pellets. A probable mechanism for porosity formation within the germ mass during the forming process, facilitated by heat-power spraying of wet charge onto the pelletizer skull, is meticulously outlined. Further, the paper delves into the potential of shaping the structural properties of iron ore pellets by manipulating the parameters of the germ mass through this technology, alongside the selection of appropriate technological characteristics for the sprayed material. The conducted research substantiates the involvement of the shear mechanism and the movement of mobile charge pulp in the formation of germs' porosity, which is predicated on the dynamic influence of the air-charge jet on wet charge materials.

References / Список литературы

1. Pavlovets V.M. Pellets in Technology of Metals Extraction from Ores. Moscow, Vologda: Infra-Ingineriya; 2022:284.

   Павловец В.М. Окатыши в технологии экстракции металлов из руд. Москва, Вологда: Инфра-Инженерия; 2022:284.

2. Pavlovets V.M. Refractory and Heat-Insulating Materials. Novokuznetsk: SibSIU; 2015:334.

   Павловец В.М. Огнеупорные и теплоизоляционные материалы. Новокузнецк: СибГИУ; 2015:334.

3. Pivinskii Yu.E., Rozhkov E.V. Ceramic castables – final stage in the evolution of low-cement refractory castables. Part 3. *Refractories and Industrial Ceramics*. 2003;44(3):134–140. https://doi.org/10.1023/A:1026391915300

4. Abzalov V.M., etc. Physico-Chemical and Thermal Engineering Fundamentals for Iron Ore Pellets Production. Ekaterinburg: NPVP "TOREX"; 2012:340.

   Абзалов В.М. и др. Физико-химические и теплотехнические основы производства железорудных окатышей. Екатеринбург: НПВП «ТОРЕКС»; 2012:340.

5. Okeke S.I., Onukwuli O.D. Effect of basicity on metallurgical properties of pellets produced from Itakpe iron ore concentrates. *Discovery and Innovation*. 1999;11(3):170–176. https://doi.org/10.4314/dai.v11i3.15549

6. Frantes K. North American iron mines running flat out to meet domestic and worldwide demand. *Skillings' Mining Review*. 2005;94(7):6–21.

7. Basics in Mineral Processing. Metso: Outotec, 2015:752. Available at URL: https://www.metso.com/globalassets/insights/ebooks/mo-basics-in-mineral-processing-handbook_lowres.pdf

8. Pavlovets V.M. Expanding the Functionality of Units for Preparing Iron Ore Raw Materials for Metallurgical Smelting. Moscow, Vologda: Infra-Ingineriya, 2023:328.

   Павловец В.М. Расширение функциональных возможностей агрегатов для подготовки железорудного сырья к металлургической плавке. Москва, Вологда: Инфра-Инженерия, 2023:328.

9. Pavlovets V.M. Development of Equipment and Technology for Pelletizing Iron Ore Raw Materials in Metallurgy. Moscow, Vologda: Infra-Engineering; 2022:336.

   Павловец В.М. Развитие техники и технологии окомкования железорудного сырья в металлургии. Москва, Вологда: Инфра-Инженерия; 2022:336.

10. Pavlovets V.M. Formation of the structure of iron ore pellets produced using heat-spraying of wet charge. *Izvestiya. Ferrous Metallurgy*. 2016;59(12):857–863. (In Russ.). https://doi.org/10.17073/0368-0797-2016-12-857-863

    Павловец В.М. Формирование структуры железорудных окатышей, полученных с использованием теплосилового напыления влажной шихты. *Известия вузов. Черная металлургия*. 2016;59(12):857–863. https://doi.org/10.17073/0368-0797-2016-12-857-863

11. Kudinov V.V., Bobrov G.V. Spray Coating, Theory, Technology and Equipment. Moscow: Metallurgiya; 1992:412.

Кудинов В.В., Бобров Г.В. Нанесение покрытий напылением, теория, технология и оборудование. Москва: Металлургия; 1992:412.

12. Baldaev L.Kh., etc. Thermal Spraying. Moscow: Market DS; 2007:344.

Балдаев Л.Х. и др. Газотермическое напыление. Москва: Маркет ДС; 2007:344.

13. Poveromo J.J. Grade pellet quality and supply. AISTech (Assoc. Iron & Steel Technology). Annual Meeting. Indianapolis; 2015:751–762.

14. Forsmo S.P.E., Samskog P.O., Bjorkman M.T. A study on plasticity and compression strength in wet iron ore green pellets related to real process variations in raw material fineness. *Powder Technology*. 2008;181(3):321–330. https://doi.org/10.1016/j.powtec.2007.05.023

15. Wang Z.C., Chu M.S., Chen S.Q., Liu Z.G., Tang J., Xue X.X. Effects of B-Mg additive on metallurgical properties of oxidized pellets. *Advanced Materials Research*. 2011;284–286:1232–1236. https://doi.org/10.4028/www.scientific.net/AMR.284-286.1232

16. Gnezdovets A.G., Kalita V.I. Model of formation of coatings macrostructure during plasma spraying. *Fizika i khimiya obrabotki materialov*. 2007;(1):30–39. (In Russ.).

Гнездовец А.Г., Калита В.И. Модель формирования макроструктуры покрытий при плазменном напылении. *Физика и химия обработки материалов*. 2007;(1):30–39.

17. Калита В.И., Комлев Д.И. Механизм формирования аморфной структуры в металлических сплавах при плазменном напылении. *Металлы*. 2003;(6):30–37.

Kalita V.I., Komlev D.I. Mechanism of formation of an amorphous structure in metal alloys during plasma spraying. *Metally*. 2003;(6):30–37. (In Russ.).

18. Goejen J.G., Miller R.A., Brindley W.J., Leissler G.W. A simulation technique for predicting defects of thermal sprayed coatings: NASA Technical Memorandum TM-106939, 1995.

19. Hansbo A., Nylén P. Models for the simulation of spray deposition and robot motion optimization in thermal spraying of rotating objects. *Surface and Coatings Technology*. 1999;122(3-4):191–201. https://doi.org/10.1016/S0257-8972(99)00255-8

20. Ensz M.T., Griffith M.L., Reckaway D.E. Critical issues for functionally graded material deposition by laser engineered net shaping. Available at URL: http://edge.cs.drexel.edu/GICL/people/schroeder/referen ces/mpif02me.pdf

21. De Los Santos Valladares L., Domínguez A.B., Félix L.L., Kargin J.B., Mukhambetov D.G., Kozlovskiy A.L., Moreno N.O., Santibañez J.F., Cabrera R.C., Barnes C.H.W. Characterization and magnetic properties of hollow α-Fe_2O_3 microspheres obtained by sol gel and spray roasting methods. *Journal of Science: Advanced Materials and Devices*. 2019;4(3):483–491. https://doi.org/10.1016/j.jsamd.2019.07.004

22. Kamijo C., Hara M., Kawaguchi T., etc. Sinter feed granulation improvement technique by pan pelletizer. *Zairyo to Prosesu = CAMP ISIJ*. 2010;23(1):5.

23. Watanabe K., Yasukawa M., Kamisaka C., etc. Improvement of productivity by installing P-type separate granulation process at Wakayama no. 5 sintering plank. *Zairyo to Prosesu = CAMP ISIJ*. 2010;23(1):6.

Information about the Author

Viktor M. Pavlovets, *Cand. Sci. (Eng.), Assist. Prof. of the Chair "Thermal Power and Ecology",* Siberian State Industrial University
E-mail: pawlowets.victor@yandex.ru

Сведения об авторе

Виктор Михайлович Павловец, *к.т.н., доцент кафедры теплоэнергетики и экологии,* Сибирский государственный индустриальный университет
E-mail: pawlowets.victor@yandex.ru

Received 11.05.2022
Revised 16.11.2022
Accepted 11.12.2023

Поступила в редакцию 11.05.2022
После доработки 16.11.2022
Принята к публикации 11.12.2023